Supporting Information

HyNA-LDI-MS: A Real-Time Mass Spectrometric Approach for Probing Interfacial Charge Transfer

Yanyan Li[1], Yang Li[2], Dingyitai Liang[1], Shouzhi Yang[1], Zhiqiang Wang[3], Xueqing Gong[2], Yuning Wang[1*], Kun Qian[1*]*

[1]State Key Laboratory of Systems Medicine for Cancer, School of Biomedical Engineering, Institute of Medical Robotics and Shanghai Academy of Experimental Medicine, Shanghai Jiao Tong University, Shanghai 200030, P. R. China

[2]State Key Laboratory of Synergistic Chem-Bio Synthesis, School of Chemistry and Chemical Engineering, Shanghai Jiao Tong University, Shanghai 200240, P. R. China

[3]State Key Laboratory of Green Chemical Engineering and Industrial Catalysis, Centre for Computational Chemistry and Research Institute of Industrial Catalysis, School of Chemistry and Molecular Engineering, East China University of Science and Technology, Shanghai 200237, P. R. China

*E-mail: xqgong@sjtu.edu.cn (X.G.), yuningwang@sjtu.edu.cn (Y.W.), k.qian@sjtu.edu.cn (K.Q.)

Method

Chemical and reagents

Chemicals and reagents in this work included reagents for the preparation of substrate materials and metabolites. For the preparation of substrate materials, chloroauric acid ($HAuCl_4 \cdot 4H_2O$, 47.8%), 1,2-dichloroethane (DCE, 99%), sodium citrate (SC, 99%), and β-cyclodextrin (β-CD, 98%) were purchased from Sinopharm Chemical Reagent Co. Ltd. (Beijing, China). Titanium alkoxide (TBOT, 95%), dopamine (DA, 98%), and anhydrous ethanol (EtOH, 99.5%) were purchased form Sigma-Aldrich (St. Louis, MO). α-Cyano-4-hydroxy-cinnamic acid (CHCA) and 2,5-dihydroxybenzoic acid (DHB) were purchased from Bruker (Bremen, Germany). Trifluoroacetic acid (TFA, 99%) and acetonitrile (ACN, 99%) were purchased from Macklin Biochemical (Shanghai, China).

For the preparation of metabolites, D-glucose (99%), L-arginine (98%), L-histidine (99.5%), sucrose (99.5%), L-cysteine (99%), L-glutathione (98%), L-methionine (99%), D-levulose (99%), α-lactose (98%), L-glutamine (99%), L-serine (99%), L-threonine (99%), L-glutamic acid (99%), L-aspartic acid (99%), L-arginine (99%), L-lysine (98%), L-phenylalanine (99%), L-tyrosine (99%), dimethylhippuric acid (96%), and adenosine (99.5%) were purchased from Sigma-Aldrich (St. Louis, MO). Juglone (5-hydroxy-1,4-naphthoquinone, ≥95%) and ascorbic acid (AA, 99%) were purchased from Macklin Biochemical (Shanghai, China). 4-methylbenzylpyridinium ion (4-MeBP) was obtained from Yeasen Biotechnology (Shanghai, China).

Synthesis of negatively charged Au nanoparticles (Au(-) NPs)

Au(-) NPs (average diameter: 15.14 nm) were synthesized as described previously.[1] In brief, 50 mL of 1 mM $HAuCl_4$ solution was brought to a boil under vigorous stirring, followed by the rapid addition of 5 mL of 38.8 mM sodium citrate. The solution was boiled for 10 min and stirred for an additional 15 min at room temperature (RT).

Synthesis of β-CD modified AuNPs

β-CD modified Au NPs (Au@ β-CD) were synthesized following a previously reported method.[2] Briefly, 5 mL of PBS (0.1 M, pH 7.0) and 10 mL of β-CD (10 mM) were added to 35 mL of 0.29 mM $HAuCl_4$ solution. The mixture was heated to boiling under vigorous stirring for 1 h. The resulting Au@ β-CD NPs solution was purified by centrifugation at 7500 rpm for 6 min in 25 mL of water.

Synthesis of TiO_2@DA NPs

Amorphous TiO_2 NPs were synthesized from titanium alkoxide (TBOT) via a sol-gel method.[3] A solution of 1 mL TBOT in 50 mL anhydrous ethanol was slowly added dropwise (1 drop/s) to a mixture of 50 mL anhydrous ethanol and 50 mL DI water under vigorous stirring. Following the addition, hydrolysis and polymerization occurred, forming a sol. After aging at RT for 1 h, a TiO_2 precursor gel precipitated. The precipitate was centrifuged and washed by ethanol. The TiO_2 NPs were obtained after drying at 60 °C for 6 h, and calcining at 320 °C for 2 h.

The surface of TiO_2 was functionalized with dopamine (DA). The preparation process was as follows: 3.0 g of TiO_2 and an appropriate amount of absolute ethanol (as solvent)

were placed into a 250 mL three-necked flask, and the TiO_2 was completely dispersed by ultrasonication. 0.3 g of DA was dissolved in 50 mL of hot ethanol solution, and then this solution was gradually added dropwise into the 250 mL three-necked flask using a 60 mL constant pressure dropping funnel, with the addition time controlled between 15 and 20 minutes. The reaction was carried out under a nitrogen atmosphere at 50 °C with magnetic stirring for 6 hours. After the reaction, a light-yellow solid powder was obtained by filtration, washing, and subsequent drying at 50 °C for 24 hours.

Fabrication of TiO_2@Au hybrid nanoarrays (HyNAs)

Two types of TiO_2@Au HyNAs were fabricated by self-assembly of Au and TiO_2 NPs with different modifications at oil-water interfaces, forming conductive NAs (Con-NAs) and insulating NAs (In-NAs). In a 500 μL of DCE system, 30 μL of Au(-) or Au@ β-CD NPs was added, followed by the addition of 30 μL of TiO_2@DA NPs. The mixture was shaken vigorously for 30 s, forming a spherical water droplet at the DCE-water interfaces. Due to their electrostatic interaction between oppositely charged NPs or host-guest interaction between β-CD and DA, Con-NAs and In-NAs were obtained, respectively. The self-assembled nanofilm was transferred to silicon wafers using the protocol described by Cecchini et al.[4] A micropipette was used to discard 100 μL of the aqueous phase to enhance particle density at the liquid-liquid interface. The entire water droplet was then transferred to a freshly cleaned silicon wafer (5 mm × 5 mm) prepared using piranha solution (30% H_2O_2/H_2SO_4, v/v = 1:3).

Characterization of the TiO_2/Au HyNAs

The obtained nanofilms on silicon wafers were characterized by scanning electron microscopy (SEM) using an S-4800 (Hitachi, Japan). Absorbance spectra were measured with a UV-2550 UV-vis spectrometer (Shimadzu, China), with nanofilms transferred to quartz sheets for analysis. Zeta potential measurements were performed on a Nano-ZS90 (Malvern, UK) by dispersing the materials in water. Photocurrent measurements were conducted in a standard three-electrode system using the HyNA on ITO conducting glass as the working electrode, platinum wire as the counter electrode, Ag/AgCl as the reference electrode, and 0.5 M Na_2SO_4 as the electrolyte. The setup utilized a CHI 660E electrochemistry workstation (ChenHua Instruments Co., China). Photoluminescence (PL) spectra were recorded on a HITACHI F4600 spectrometer with 355 nm excitation. Bright-field images of the sample-matrix crystallization were captured using the Nikon Eclipse Ti microscope (Nikon Ltd., Japan), while high-resolution 3D topography data were acquired with the KEYENCE VK-X3000 laser confocal scanning microscope (KEYENCE Ltd., Japan) to analyze the surface flatness of the nanostructures. X-ray photoelectron spectroscopy (XPS) was performed on a Perkin-Elmer PHI 5000C ESCA system with AI Kα radiation operated at 250 W. The FLIR T800 thermal camera was used to monitor temperature variations during UV light exposure.

Theoretical calculations

Simulations were conducted using the finite element method (FEM) with COMSOL Multiphysics 6.0 to study the electromagnetic and temperature field distributions on TiO_2 NPs, Au NPs, and HyNA surfaces under 355 nm laser excitation. The HyNA model consisted

of a 3 × 3 array of TiO_2 and Au NPs, with interparticle distances of 1 nm (TiO_2 and Au), 3 nm (Au and Au), and 3 nm (TiO_2 and TiO_2). The physical parameters of AuNPs and TiO_2 NPs were defined based on previous reports.[5] The incident laser parameters were aligned with those of the LDI-MS instrument used in this study. An ambient temperature of 293 K was set to calculate the surface temperature distribution.

The adsorption energy calculations were carried out within the density function theory (DFT) by the Vienna ab initio simulation package (VASP).[6, 7] The generalized gradient approximation (GGA) was applied by using the Perdew, Burke, and Ernzerhof functional (PBE)[8] to reliably calculate the electronic exchange and correlation, with a cut-off energy of 400 eV for the plane-wave basis set expansion. The project-augmented wave (PAW) method was used to represent the core-valence electron interaction. The calculations were also conducted involving on-site Coulomb corrections (DFT+U, U = 4.2 eV for Ti 3d orbitals)[9] as well as long-range dispersion interactions (DFT-D).[10] The dispersion correction method, DFT-D3 method with Becke-Johnson damping function was applied to reliably calculate the van der Waals (vdW) interactions resulting from long-term interactions.

For the model construction, a p(4×2) surface slab with three O-Ti-O atomic layers was built for the rutile TiO_2(110) surface. The top two layers of the slabs were allowed to fully relax, while the bottom layer was kept fixed to mimic the bulk region; and a vacuum gap of 20 Å was used to eliminate the interaction between neighboring slabs. Moreover, the Au(111) and Au(511) surface were modeled by a p(6×6) supercell and a p(2×4) supercell

with four atom layers, respectively. Both the top three layers of the slabs were allowed to fully relax, while the bottom layer was kept fixed to mimic the bulk region.

The adsorption energies were calculated by the following equation:

$$E_{ads} = -(E_{glu/M} - E_{glu} - E_M)$$

where E_{ads} represents the adsorption energy; $E_{glu/M}$ is the total energy of the adsorbed glucose at adsorbent M (Au/TiO_2); E_{glu} and E_M are energies for glucose and rutile TiO_2(110), Au(111) and Au(511) surfaces, respectively. For the calculations of adsorption on surfaces, a Monkhorst-Pack grid of (1×1×1) k points was used for Brillouin-zone integrations.

Different adsorption configurations were considered in all calculations. O atom from the hemiacetal and from the hydroxyl group were considered for bonding to the surface, respectively. And two adsorption modes: vertical and parallel, were investigated in this work. Only stable adsorption structures were demonstrated, others showed less possibilities to maintain their structures.

LDI-MS analysis

For preparation of mass spectrometric monitoring of charge transfer and heat dissipation processes, a concentration gradient of juglone solutions was prepared in anhydrous acetonitrile, spanning four orders of magnitude from 10 mM to 0.01 mM. AA was dissolved in ultrapure water to obtain a 10 mM aqueous solution. 4-MeBP was prepared as a 1 mM solution in acetonitrile.

For metabolite detection, standard small molecules (D-glucose, L-arginine, L-histidine, sucrose, L-cysteine, L-glutathione, L-methionine, D-levulose, α-lactose, L-glutamine, L-serine, L-threonine, L-glutamic acid, L-aspartic acid, L-arginine, L-lysine, L-phenylalanine, L-tyrosine, dimethylhippuric acid, and adenosine) were dissolved in DI water at a concentration of 1 mM. Serum samples were diluted ten fold with DI water prior to detection.

To determine the limit of detection (LOD) of the Con-NA, D-glucose concentrations ranging from 10 μM to 1 mM were analyzed. Linear regression analysis was performed to establish the regression equation correlating intensity with concentration data.[11] The LOD for the Con-NA was calculated using the slope of the regression equation along with a signal-to-noise ratio (S/N) of 3.

In LDI-MS experiments, 1 μL of the analyte solution was spotted on the HyNAs. Mass spectra were recorded on the AutoFlex (Time of Flight-Mass Spectrometry, TOF-MS, Bruker, Germany) with a Nd:YAG laser (355 nm). The acquisitions were conducted in positive mode using delayed extraction, featuring a repetition rate of 1000 Hz and an acceleration voltage of 20 kV. The optimized delay time for this experiment was set at 150 ns. Each analysis comprised 2000 laser shots.

Clinical sample collection for Con-NAs based LDI-MS application

Serum samples were collected from renal carcinoma (RCC) patients, benign prostatic hyperplasia (BPH) patients, patients with other urinary system diseases, and healthy controls (HCs) at Renji Hospital, affiliated with Shanghai Jiao Tong University School of

Medicine. The cohort included 40 RCC patients, 20 BPH patients, 30 patients with other urinary system diseases, and 40 HCs (detailed in Table S2). This study adhered to the principles of the Declaration of Helsinki, with protocols approved by the ethics committee of Renji Hospital (IRB KY2022-001-B). Written informed consent was obtained from all participants or their authorized representatives before any study procedures.

Blood samples were collected in the morning after overnight fasting from each patient and healthy volunteer, following strict protocols.[12] For serum sample harvesting, collected peripheral venous blood samples were transferred to vacuum blood collection tubes without anticoagulants and allowed to clot at room temperature for 1 h. The blood was then centrifuged at 5000 g for 10 min at 4 °C to obtain the supernatant serum samples, which were stored at -80 °C until use.

For LDI detection, the HyNA was first transferred onto the target plate. Subsequently, 1 μL of the 10-fold diluted serum sample was spotted onto the HyNAs and air-dried prior to LDI-MS analysis.

Data analysis

The MS spectra analysis in this work included data preprocessing and machine learning. For data processing of mass spectra, spectral smoothing and baseline correction were performed to eliminate noise in raw mass spectra. Subsequently, the m/z signals with S/N ≥3 were extracted from mass spectra in peak detection. Finally, peak alignment was performed to align the same m/z signal across different samples. The machine learning of serum metabolic fingerprints was performed using the Orange software (version 3.33.0,

Slovenia).[13] Initially, all the samples were tested using 5-fold cross-validation to determine the machine learning model in neural network. The performance was evaluated based on metrics including area under the curve (AUC), sensitivity, and specificity.

Supplementary figures

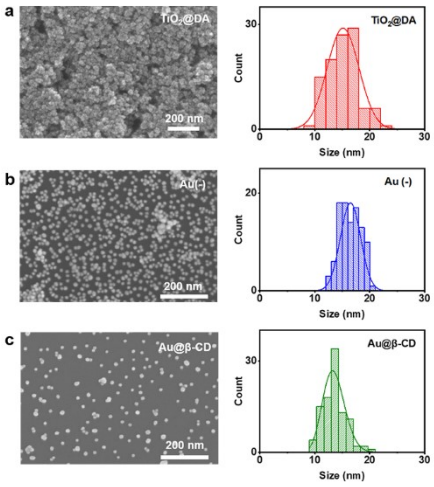

Figure S1. SEM images and size distribution of (a)TiO_2@DA NPs, (b) Au(-) NPs, (c) Au@ β-CD NPs.

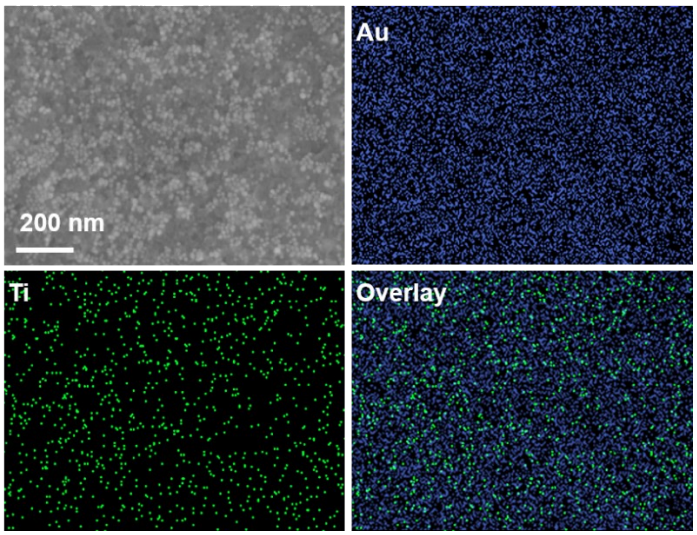

Figure S2. Elemental mapping analysis of Con-NA.

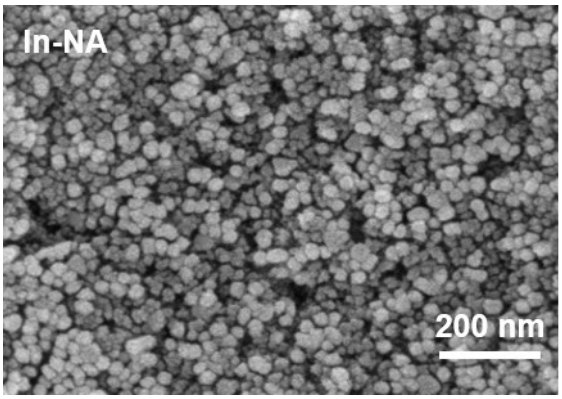

Figure S3. SEM image of In-NA.

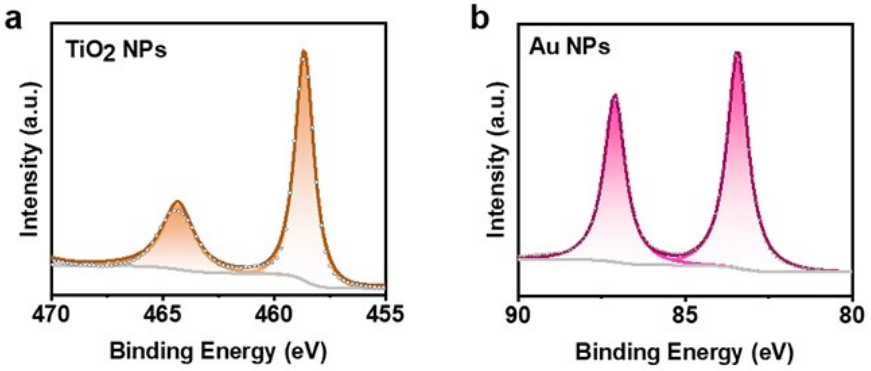

Figure S4. The XPS high-resolution spectra of (a) TiO_2 NPs for Ti2p and (b) Au NPs for Au4f.

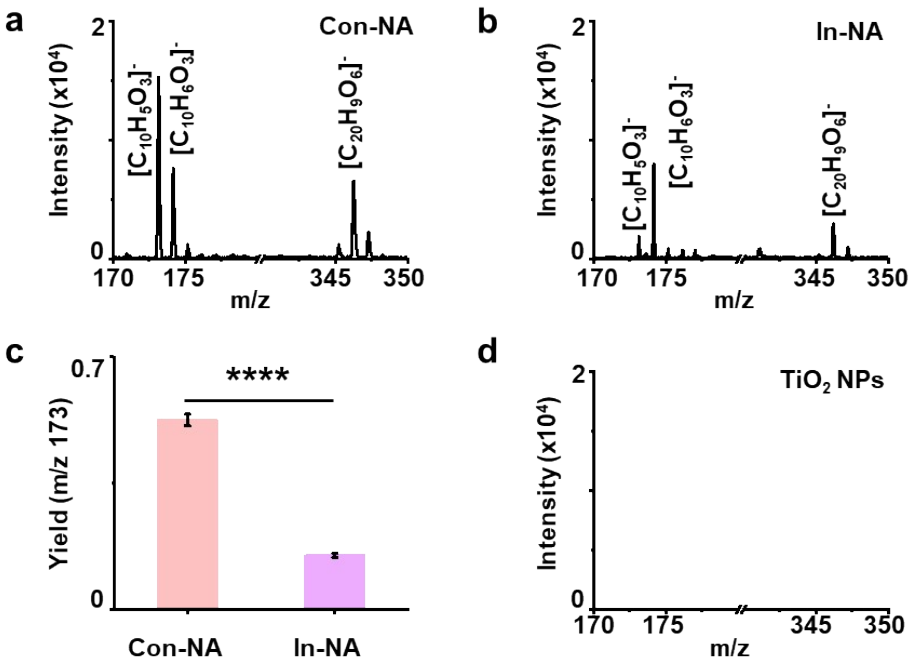

Figure S5. The mass spectra of juglone based on (a) Con-NA and (b) In-NA at the negative mode. (c) The yield of juglone anions at m/z 173.02. (d) The mass spectrum of juglone based on TiO_2 NPs at the negative mode.

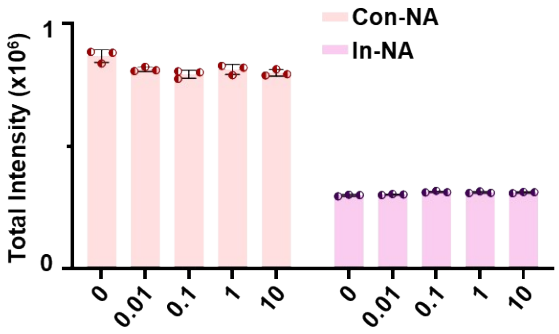

Figure S6. The 4-MeBP total intensity of Con-NA and In-NA with the increase of juglone amount.

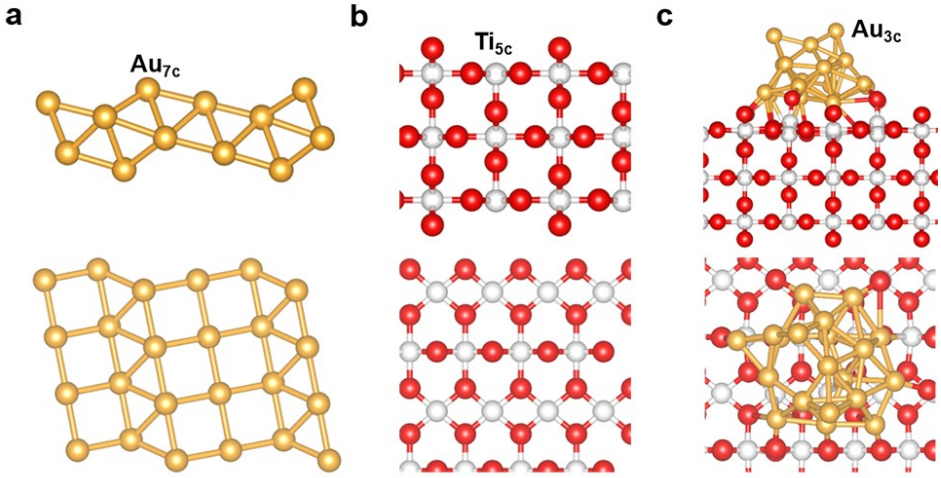

Figure S7. Calculated structures (top: side view; bottom: top view) of the (a) Au(511), (b) rutile TiO_2(110), and (c) $Au_{20}TiO_2$(110) surfaces. Red: O atoms; white: Ti atoms; blonde: Au atoms. These notations are used throughout the paper.

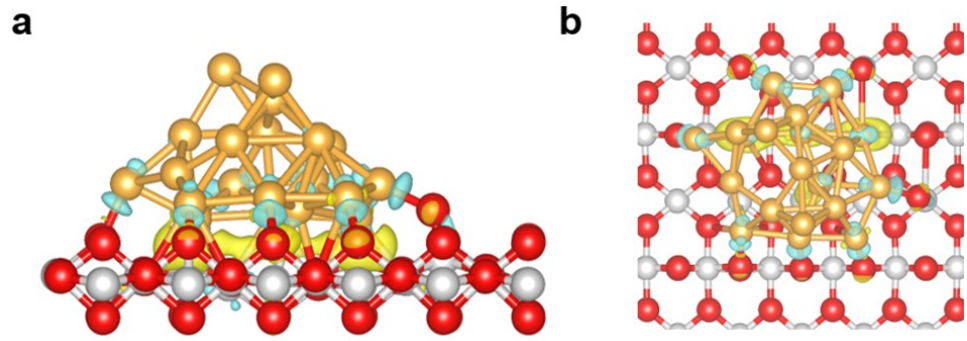

Figure S8. Calculated charge density difference (left: side view; right: top view) of the $Au_{20}TiO_2(110)$ surfaces. The isosurface is 0.05 eV/Å^3.Yellow and cyan represent electron accumulation and electron depletion, respectively.

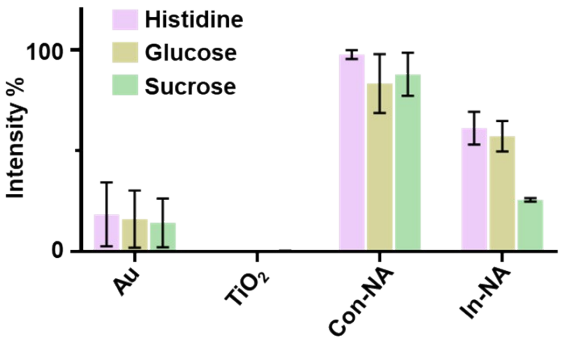

Figure S9. The LDI-MS performance of Au NPs, TiO_2 NPs, Con-NA, and In-NA for analysis of histidine, D-glucose, and sucrose (1 mM for each).

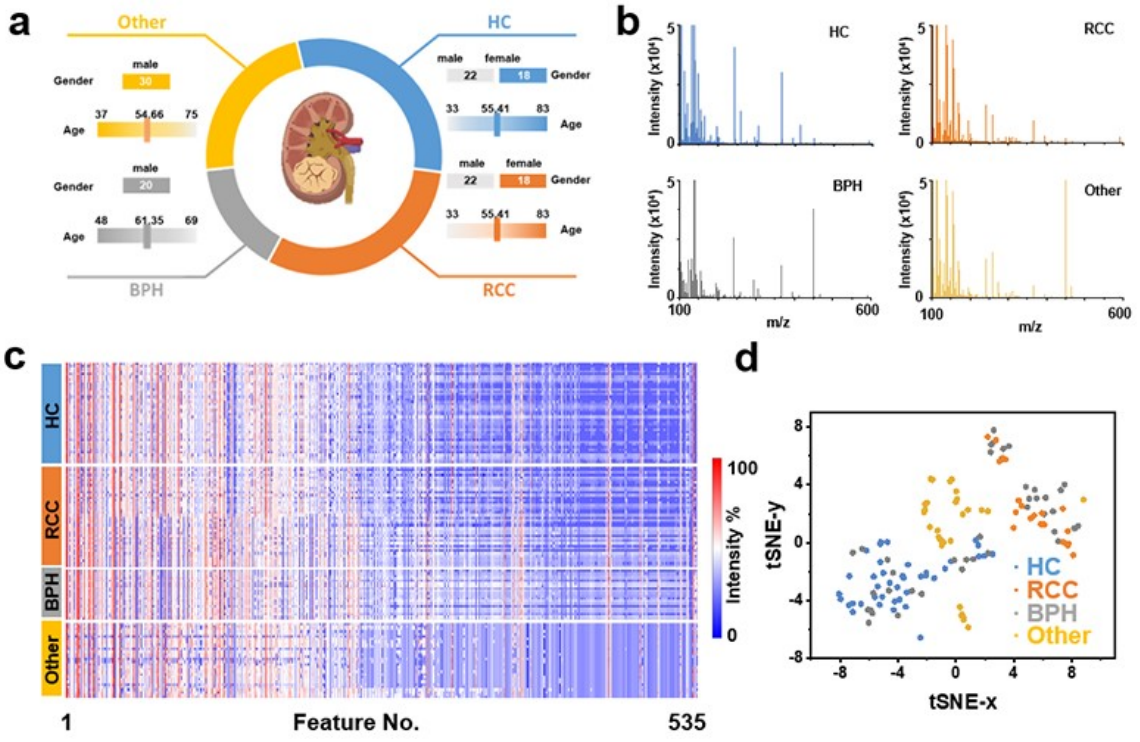

Figure S10. (a) The gender and age distribution of healthy controls (HCs), renal cell carcinoma patients (RCC patients), prostatic hyperplasia (BPH patients), and other urinary system disease patients (40/40/20/30). (b) The typical serum MS spectra at m/z 100-600 based on TiO_2/Au Con-NA. (c) The heatmap of serum metabolic fingerprints (SMFs) extracted from raw MS data including 535 features. (d) tSNE visualization of the cluster results of the HC (blue), RCC (orange), BPH (gray), and other urinary system disease patients (yellow) groups.

Supplementary tables

Table S1. The unit cell parameters and original parameters of rutile TiO_2 and Au calculated.

Unit cell	direction	Original value(Å)	Calculated value(Å)	Relative error (%)
Au	X	4.07830	4.12694	1.19
	Y	4.07830	4.12694	1.19
	Z	4.07830	4.12693	1.19
rutile TiO_2	X	4.59400	4.54635	1.04
	Y	4.59400	4.54635	1.04
	Z	2.95900	2.99746	1.30

Table S2. The sample information of patients.

Clinical indexes	HC Group (n=40)	RC Group (n=40)	BPH Group (n=20)	Other Group (n=30)
Age (Years)	52.25±13.67	55.02±11.93	61.35±5.32	54.67±10.25
Gender (Male/Female)	22/18	23/17	20/NA	30/NA

Reference

(1) Wang, Y.; Zhang, K.; Tian, T.; Shan, W.; Qiao, L.; Liu, B. Self-assembled au nanoparticle arrays for precise metabolic assay of cerebrospinal fluid. *ACS Appl. Mater. Interfaces* 2021, *13* (4), 4886-4893.

(2) Wang, Y.; Liu, Y.; Yang, S.; Yi, J.; Xu, X.; Zhang, K.; Liu, B.; Qian, K. Host–guest self-assembled interfacial nanoarrays for precise metabolic profiling. *Small* 2023, *19* (51), 2207190.

(3) Li, Z.; Zhu, Y.; Wang, J.; Guo, Q.; Li, J. Size-controlled synthesis of dispersed equiaxed amorphous TiO_2 nanoparticles. *Ceram. Int.* 2015, *41* (7), 9057-9062.

(4) Cecchini, M. P.; Turek, V. A.; Paget, J.; Kornyshev, A. A.; Edel, J. B. Self-assembled nanoparticle arrays for multiphase trace analyte detection. *Nat. Mater.* 2013, *12* (2), 165-171.

(5) Yao, G.; Liu, Q.; Zhao, Z. Studied localized surface plasmon resonance effects of Au nanoparticles on TiO_2 by FDTD simulations. *Catalysts* 2018, *8* (6), 236.

(6) Kresse, G.; Furthmüller, J. Efficiency of ab-initio total energy calculations for metals and semiconductors using a plane-wave basis set. *Comput. Mater. Sci.* 1996, *6* (1), 15-50.

(7) Kresse, G.; Furthmüller, J. Efficient iterative schemes for ab initio total-energy calculations using a plane-wave basis set. *Phys. Rev. B* 1996, *54* (16), 11169-11186.

(8) Perdew, J. P.; Burke, K.; Ernzerhof, M. Generalized gradient approximation made simple. *Phys. Rev. Lett.* 1996, *77* (18), 3865-3868.

(9) Deskins, N. A.; Rousseau, R.; Dupuis, M. Distribution of Ti^{3+} surface sites in reduced TiO_2. *J. Phys. Chem. C* 2011, *115* (15), 7562-7572.

(10) Grimme, S. Semiempirical GGA-type density functional constructed with a long-range dispersion correction. *J. Comput. Chem.* 2006, *27* (15), 1787-1799.

(11) Arendowski, A.; Nizioł, J.; Ruman, T. Silver-109-based laser desorption/ionization mass spectrometry method for detection and quantification of amino acids. *J. Mass Spectrom.* 2018, *53* (4), 369-378.

(12) Yang, J.; Wang, R.; Huang, L.; Zhang, M.; Niu, J.; Bao, C.; Shen, N.; Dai, M.; Guo, Q.; Wang, Q.; et al. Urine metabolic fingerprints encode subtypes of kidney diseases. *Angew. Chem. Int. Ed.* 2020, *59* (4), 1703-1710.

(13) Demšar, J.; Curk, T.; Erjavec, A.; Gorup, C.; Zupan, B. Orange: Data mining toolbox in python. *J. Mach. Learn. Res.* 2013, *14* (1), 2349-2353.